PCP
PLANT & CELL PHYSIOLOGY

The Deconstruction of Pectic Rhamnogalacturonan I Unmasks the Occurrence of a Novel Arabinogalactan Oligosaccharide Epitope

Fanny Buffetto[1,4], Valérie Cornuault[2], Maja Gro Rydahl[3], David Ropartz[1], Camille Alvarado[1], Valérie Echasserieau[1], Sophie Le Gall[1], Brigitte Bouchet[1], Olivier Tranquet[1], Yves Verhertbruggen[1], William G.T. Willats[3], J. Paul Knox[2], Marie-Christine Ralet[1] and Fabienne Guillon[1,*]

[1]INRA, UR1268 Biopolymères Interactions Assemblages, 44300 Nantes, France
[2]Centre for Plant Sciences, Faculty of Biological Sciences University of Leeds, Leeds LS2 9JT, UK
[3]Department of Plant and Environmental Sciences, University of Copenhagen, 1871 Frederiksberg, Denmark
[4]Present address: Institute for Wine Biotechnology, Department of Viticulture and Oenology, Faculty of AgriSciences, Stellenbosch University, Matieland 7602, South Africa.
*Corresponding author: E-mail, fabienne.guillon@nantes.inra.fr
(Received June 22, 2015; Accepted September 2, 2015)

Rhamnogalacturonan I (RGI) is a pectic polysaccharide composed of a backbone of alternating rhamnose and galacturonic acid residues with side chains containing galactose and/or arabinose residues. The structure of these side chains and the degree of substitution of rhamnose residues are extremely variable and depend on species, organs, cell types and developmental stages. Deciphering RGI function requires extending the current set of monoclonal antibodies (mAbs) directed to this polymer. Here, we describe the generation of a new mAb that recognizes a heterogeneous subdomain of RGI. The mAb, INRA-AGI-1, was produced by immunization of mice with RGI oligosaccharides isolated from potato tubers. These oligomers consisted of highly branched RGI backbones substituted with short side chains. INRA-AGI-1 bound specifically to RGI isolated from galactan-rich cell walls and displayed no binding to other pectic domains. In order to identify its RGI-related epitope, potato RGI oligosaccharides were fractionated by anion-exchange chromatography. Antibody recognition was assessed for each chromatographic fraction. INRA-AGI-1 recognizes a linear chain of (1→4)-linked galactose and (1→5)-linked arabinose residues. By combining the use of INRA-AGI-1 with LM5, LM6 and INRA-RU1 mAbs and enzymatic pre-treatments, evidence is presented of spatial differences in RGI motif distribution within individual cell walls of potato tubers and carrot roots. These observations raise questions about the biosynthesis and assembly of pectin structural domains and their integration and remodeling in cell walls.

Keywords: AGI • INRA-AGI-1 • Plant cell wall • Rhamnogalacturonan I • *Solanum tuberosum*.

Abbreviations: AGI, type I arabinogalactan; AGII, type II arabinogalactan; Ara, arabinose; BSA, bovine serum albumin; DP, degree of polymerization; ELISA, enzyme-linked immunosorbent assay; EDC, epitope detection chromatography; Gal, galactose; GalA, galacturonic acid; HG, homogalacturonan; LC-MS, liquid chromatography–mass spectrometry; mAb, monoclonal antibody; MS/MS, tandem mass spectrometry; PBS, phosphate-buffered saline; Rha, rhamnose; RGI, rhamnogalacturonan I; RUP oligosaccharides, RGI oligosaccharides derived from potato tuber.

Introduction

Rhamnogalacturonan I (RGI) accounts for 20–35% of pectic polysaccharides (Mohnen 2008) and is one of the most heterogeneous polysaccharides found in plant cell walls. Its backbone is composed of [→2)-α-L-Rha*p*-(1→4)-α-D-GalA*p*-(1→] repeats. Uronic acids from RGI can be acetylated at the *O*-2 and *O*-3 position. Around 20–80% of the Rha*p* residues can be substituted at *O*-4 and, to a lower extent, at *O*-3 with neutral side chains (Albersheim et al. 1996, Ridley et al. 2001). RGI side chains include galactan, arabinan or type I (AGI) and II (AGII) arabinogalactan (Carpita and Gibeaut 1993, Willats et al. 2001, Caffall and Mohnen 2009). Over 15 different linkages have been identified in RGI side chains (Lau et al. 1987, Caffall and Mohnen 2009). Arabinan consists of a (1→5)-α-L-Ara*f* backbone, which can be branched at *O*-3 with Ara*f* units and/or arabinan secondary side chains. Galactan and AGI are both made of a (1→4)-β-D-Gal*p* backbone on which substitutions by monomeric Gal*p* units at the *O*-6 or at the *O*-3 position can occur. AGI is further substituted with α-L-Ara*f*-*p* residues and/or with (1→5)-α-L-Ara*f* short side chains. AGII is composed of a (1→3)-β-D-Gal*p* backbone decorated with (1→6)-β-D-Gal*p* secondary chains, which are arabinosylated. According to plant sources, organs, tissues and developmental stages, RGI side chain composition, length and degree of branching are highly variable (Lerouge et al. 1993, Willats et al. 2001, Caffall and Mohnen 2009). The precise function of RGI is still under debate. Arabinan and galactan are highly mobile polymers compared with other pectin components and have been suggested to act as wall plasticizers and water-binding agents during plant

Plant Cell Physiol. 56(11): 2181–2196 (2015) doi:10.1093/pcp/pcv128, Advance Access publication on 17 September 2015, available online at www.pcp.oxfordjournals.org

growth and development (Ha et al. 2005, Larsen et al. 2011, Ng et al. 2013). Interestingly, resurrection plants, which possess the ability to survive dehydration of their vegetative organs for an extended period of time and to recover a full metabolic competence upon rehydration, show a high content of arabinose in their leaves (Moore et al. 2008, Moore et al. 2013). By extension, it has been speculated that arabinan and galactan, when abundantly present in seeds, can serve a dual function, protecting the seeds against desiccation and providing energy to the growing embryo following germination (Gomez et al. 2009). The role of arabinan in cell wall flexibility has also been demonstrated in stomatal guard cells (Jones et al. 2003, Jones et al. 2005) and epidermal stem cells (Verhertbruggen et al. 2013). Ulvskov et al. (2005) have investigated the significance of RGI structure for wall rheology, using potato tubers in which RGI structure had been remodeled in vivo using fungal enzymes. Tuber RGI molecules with reduced amounts of linear galactans and branched arabinans were more brittle when subjected to uniaxial compression. The authors suggest that the pectic matrix may play a role in transmitting stresses to the load-bearing cellulose microfibrils and that small changes to the matrix environment impact the biophysical properties of the wall. Zykwinska et al. (2005, 2006, 2007) showed that diverse pectic populations may co-exist in the cell wall, one highly mobile and the other one displaying a restricted mobility and closely associated with the cellulose surface. From these studies, it can be envisaged that some pectic side chains could tether cellulose microfibrils (Zykwinska et al. 2005, Zykwinska et al. 2006, Zykwinska et al. 2007). Pectins together with xyloglucans would control spacing between cellulose microfibrils, and thus wall extensibility. In contrast, other studies suggest that arabinan could also be involved in cell–cell adhesion (Iwai et al. 2001, Orfila et al. 2001). As a matter of fact, the exact contribution of the individual RGI domains in plant physiology remains to be clarified.

High resolution imaging with the aid of specific monoclonal antibodies (mAbs) is very helpful to place the structural complexity of cell wall polysaccharides including pectin in cell biological and developmental contexts (Willats et al. 2001). A large set of mAbs against pectin motifs is already available (e.g. through the Plant Probes and CCRC websites) amongst which several mAbs are specifically directed against RGI motifs (Jones et al. 1997, Willats et al. 1998, Clausen et al. 2003, Young et al. 2008, Verhertbruggen et al. 2009a, Ralet et al. 2010). However, antibodies directed to highly branched pectic domains or to the junction between the side chains and the RGI backbone have not yet been isolated.

Here, we describe the production and characterization of a novel mAb that binds to AGI. Its immunogen was engineered from RGI isolated from potato pulp by designing through enzymatic catalysis highly branched RGI oligosaccharides with very short side chains and conjugating these oligomers to carrier protein. Subsequent to immunization with this conjugate, we have identified a mouse mAb, designated INRA-AGI-1, which recognizes a motif with galactosyl and arabinosyl residues in a linear chain. The INRA-AGI-1 epitope is present within cell walls of potato tuber and carrot root. Pre-treatment with galactanase was required to unmask the epitope, and no strict co-localization with any of the established RGI antibody epitopes was observed. Based on our findings, we discuss RGI structure, its integration within the pectic and cell wall architectures and how mAbs coupled with enzymatic deconstruction can provide information on the biosynthesis, deposition and remodeling of plant cell wall polymers.

Results

RGI oligosaccharides from potato tuber cell walls consist of RGI stretches highly substituted with short side chains

Raw RGI was isolated from de-starched potato pulp using alkaline extraction at high temperature, and was further purified using an anion-exchange batch separation. Purified RGI was then partially depleted of arabinan and galactan side chains to produce so-called low-branched RGI. The RGI backbone was split using a rhamnogalacturonan hydrolase and the large fragments were removed by ethanol precipitation. The pool of oligosaccharides recovered in the ethanol-soluble fraction (designated RUP oligosaccharides) exhibited a galacturonic acid (GalA) over rhamnose (Rha) molar ratio of 1 : 2 and was rich in galactose (Gal) and to a lesser extent in arabinose (Ara) (**Fig. 1A**). RUP oligosaccharides also contained low amounts of glucose, fucose, mannose, xylose and glucuronic acid that probably originate from residual hemicelluloses (Cornuault et al. 2015).

The structural features of RUP oligosaccharides were further investigated by glycosidic linkage and mass spectrometry analyses. Sugar linkage analysis of RUP oligosaccharides was consistent with the neutral sugar composition determined as alditol acetates (**Fig. 1A**). Close to 50% of the Rha*p* residues were identified as 2,4-linked and 16.8% as 2-linked, showing that a high proportion of internal Rha molecules linked at *O*-2 to GalA within the RGI stretches are branched at *O*-4 with side chains. A high proportion (27.8%) of 4-linked Rha*p* was detected (**Fig. 1A**). These units are assumed to constitute the non-reducing ends of RGI fragments branched at *O*-4 with neutral sugar side chains. Finally, a low proportion of unbranched terminal Rha*p* was detected. Considering 2- and 2,4-linked Rha*p* as internal residues and t- and 4-linked Rha*p* as non-reducing termini, an average degree of polymerization (DP) of 5.7 was calculated for the RGI backbone in RUP oligosaccharides. Ara was mainly present as 1,5-linked Ara*f* and t-Ara*f* units, which is typical of linear arabinans (Khodaei and Karboune 2013). Terminal Ara*p* was also detected as previously reported in soybean RGI (Huisman et al. 2001). The ratio of 1,5-linked Ara*f* over t-Ara*f* + t-Ara*p* was close to 1. Galactose was mainly present as t-Gal*p*. The low ratio of 1,4-linked Gal*p*/t-Gal*p* (0.3) indicates that Rha*p* units mainly carry single Gal*p* units. RUP oligosaccharides also contained 1,6-Gal*p* and 1,3-Gal*p*, but these linkages were detected in very low amounts, in agreement with the findings of Khodaei and Karboune (2013).

Mass analysis of RUP oligosaccharides was performed using liquid chromatography–mass spectrometry (LC-MS) (**Fig. 1B**).

A

	Sugar residues	RUP oligo**
Neutral sugars	Rha (R)	22.7
	Ara (A)	7.9
	Gal (G)	36.7
	Glc+Fuc+Man+Xyl	2.9
Uronic acids	GalA (U)	28.3
	GlcA	1.5

Linkages	RUP	
	% Total sugar	Repartition per individual sugar
t-Rha	2.4	6.6
2-Rha	6.3	16.8
4-Rha	10.3	27.8
2,4-Rha	18.1	48.8
2,3,4-Rha	0	0
Total	37.1	100
t-Arap	4.2	30.7
t-Araf	1.8	13
5-Ara	7.8	56.3
3,5-Ara	0	0
Total	13.9	100
t-Gal	29.3	64.9
3-Gal	3	6.6
6-Gal	2.3	5.1
4-Gal	9.4	20.9
3,4-Gal	0.5	1.2
4,6-Gal	0.6	1.3
Total	45.1	100
t-Xyl	2.4	100
t-Glc	1.4	100
Total	1.4	100

B

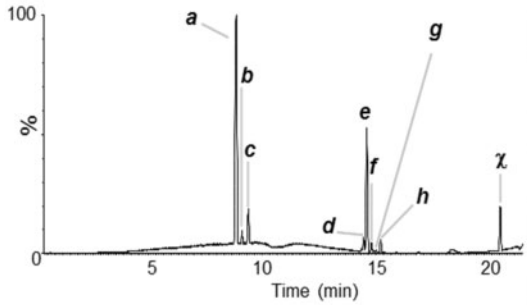

Fig. 1 Characterization of the RUP oligosaccharides. (A) Sugar composition and glycosidic linkages of RUP oligosaccharides. Both composition and linkages are given in molar percentage **Values determined by V. Cornuault (Cornuault et al. 2015). p, pyranose; f, furanose. (B) LC-MS chromatogram of RUP oligosaccharides. (a) *m/z* 985.3 $R_2U_2G_2$; (b) *m/z* 1249.4 $R_2U_2G_2A_2$ and *m/z* 823.2 $R_2U_2G_1$; (c) *m/z* 661.2 R_2U_2; (d) m/z 866.2* $R_3U_3G_3A_2$ and *m/z* 815.2* $R_3U_3G_4$; (e) *m/z* 1469.4 $R_3U_3G_3$; (f) *m/z* 1307.3 $R_3U_3G_2$; (g) *m/z* 638.2* $R_3U_3G_1A_1$ and *m/z* 1145.3 $R_3U_3G_1$; (h) *m/z* 983.2 R_3U_3. R, Rha; U, GalA; G, Gal; A, Ara; *doubly charged ions; χ, contaminant.

Eleven RGI-related oligosaccharides were detected and all encompassed a DP4 or DP6 RU backbone. The oligosaccharides with a DP4 backbone were eluted first followed by those of DP6. Two compounds could be assigned to unbranched RUP oligosaccharides, six to RUP oligosaccharides branched solely with hexoses and three others to RUP oligosaccharides branched with both hexoses and pentoses. Based on sugar composition (**Fig. 1A**), pentose is likely to be Ara and hexose is likely to be Gal. The two major compounds detected by mass spectrometry corresponded to R_nU_n (R, Rha; U, GalA; $n = 2$ or 3) oligomers with Rha residues fully substituted by Gal. $R_2U_2G_2$ (G, Gal) has been previously reported as a major compound in rhamnogalacturonan hydrolase digest of potato de-esterified modified hairy regions (Schols et al. 1994).

Considering the proportion of branched Rha*p* residues (75%) and the proportion of total Ara and Gal residues, one can assume that RUP oligosaccharides encompass DP4 and DP6 RUP oligosaccharides bearing mainly monomeric or very short Ara- and Gal-containing side chains.

Monoclonal antibodies to RUP oligosaccharides bind to galactan-rich RGI

After lymphocyte fusion with splenocytes, resulting hybridomas were screened on RUP–bovine serum albumin (BSA) and BSA. Four clone supernatants, which reacted only with RUP–BSA, were selected for further characterization. Isotyping revealed that the selected mAbs were all IgMs.

The binding of the four supernatants to a set of cell wall-derived polysaccharides and oligosaccharides was investigated using glycan microarrays (**Fig. 2A**). None of the supernatants bound to non-pectic oligosaccharides or polysaccharides printed on the array (cellulose, xylan, mannan or xyloglucan; data not shown). The four supernatants exhibited similar epitope recognition patterns, which differed widely from those obtained with well-known pectin antibodies (Liners et al. 1989, Jones et al. 1997, Willats et al. 1998, Clausen et al. 2004, Verhertbruggen et al. 2009a, Verhertbruggen et al. 2009b, Ralet et al. 2010). The two sole polysaccharides recognized by the supernatants were potato and soybean RGI. These two substrates originate from pectic galactan-rich organs (Jarvis et al. 1981, Massiot et al. 1988, Buckeridge et al. 2005). This specific binding confirmed that the epitope belongs to the RGI domain. The four antibodies all bound to the RUP oligosaccharides used for mice immunization and clone selection, but all other RGI-related oligosaccharides were not recognized. Neither linear galactan (DP2, 3, 5, 8) or arabinan (DP5, 6, 12) oligosaccharides or unbranched RGI backbone oligosaccharides were recognized by the supernatants. Interestingly, none of the supernatants reacted with $R_2U_2G_2$. Therefore, we hypothesized that the epitope corresponds to a very specific structure located either in between the RGI side chains and the backbone, or present within the side chains themselves.

In order to characterize further the recognition of the RGI epitopes by the new antibodies, competitive inhibition

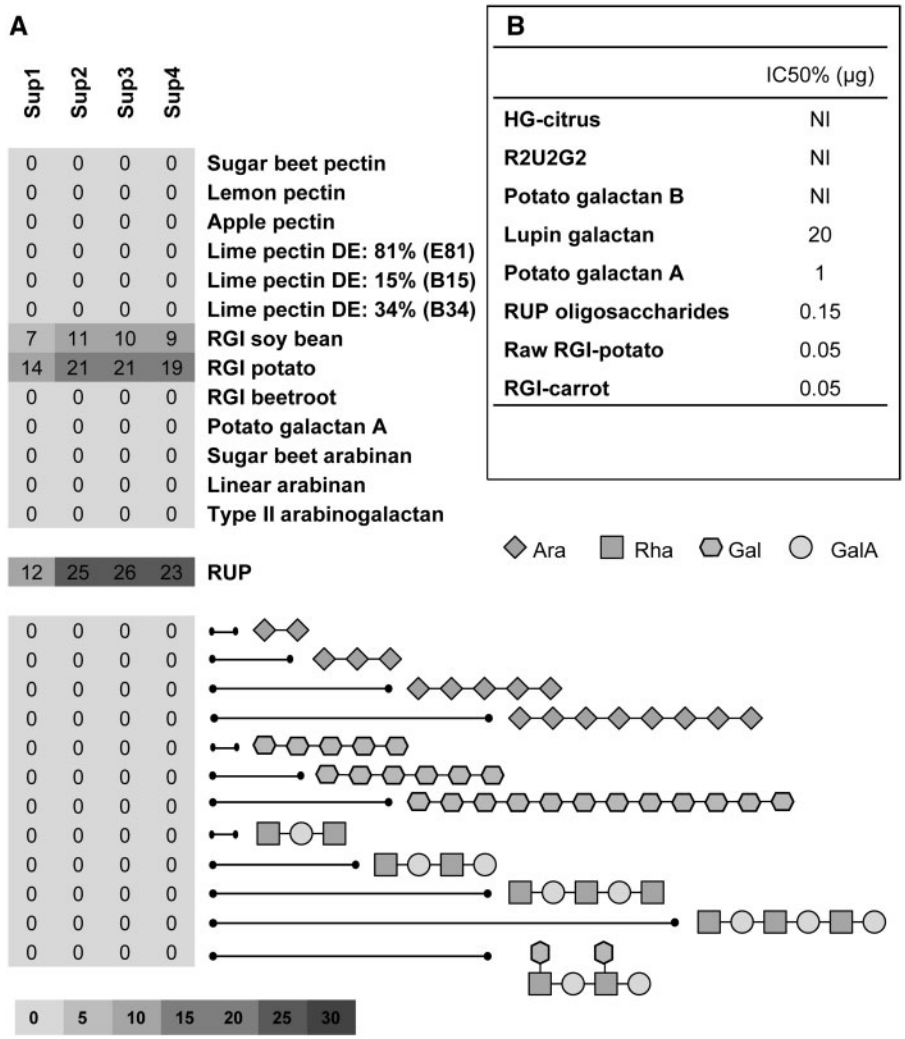

Fig. 2 Characterization of mAb specificity. (A) Four mAbs raised against RUP oligosaccharides were isolated and the binding of supernatants (Sup1–Sup4) to carbohydrate polymers and oligomers was tested using glycan microarrays. The results are shown as a percentage based on the maximal total mean sample values recorded on the array. (B) Competitive inhibition ELISA performed with the Sup2/INRA-AGI-1 antibody. IC50% is defined as the concentration of inhibitor required to give 50% inhibition of the binding of the antibody to RUP–BSA. The lower is the concentration; the upper is the avidity of the antibody for the inhibitor. NI, no inhibition.

enzyme-linked immunosorbent assays (ELISAs) were carried out using various RGI fragments isolated from pectic galactan-rich sources. In parallel, homogalacturonan (HG) extracts from citrus and $R_2U_2G_2$ were used as negative controls. Since the four mAbs exhibited similar binding profiles on microarray, only one out of the four supernatants (Sup2), which exhibited the highest binding intensity for both potato RGI and RUP oligosaccharides, was selected for further analysis. The 50% inhibitory concentration (IC_{50}) of the maximal antibody binding to RUP pool–BSA was used to compare its affinity with a range of hapten inhibitors (**Fig. 2B**). Sup2 showed a stronger affinity for potato raw RGI (IC_{50}: 0.05 µg) than for RUP oligosaccharides (IC_{50}: 0.15 µg). Carrot RGI and, to a lower extent, lupin galactan and commercial potato pectic galactan were also recognized by the antibody. Interestingly, Sup2 did not have the same affinity for the two galactan samples extracted from potato (**Fig. 2B**). The antibody only bound to the commercial galactan (galactan A), which is less pure (see **Table 2**).

Altogether, these results indicate that the epitope occurs in RGI and is strongly detected in plant extracts, such as potato pulp, which have abundant RGI galactan side chains. Unlike the purified extract of potato galactan that does not contain the epitope, less purified galactans were recognized by Sup2. Therefore, it can be hypothesized that the putative epitope involves sugars other than Gal residues.

The epitope consists of a galactan chain interspersed with a short stretch of arabinan

An epitope detection chromatography (EDC) procedure (Cornuault et al. 2014), adapted to competitive inhibition mode, was performed to pursue the epitope characterization. RUP oligosaccharides were fractionated according to their charge density by anion-exchange chromatography (**Fig. 3**). Each fraction was analyzed by colorimetry for GalA and total neutral sugar content, and tested with the Sup2 antibody using competitive inhibition ELISAs. Five pools (designed P1–P5)

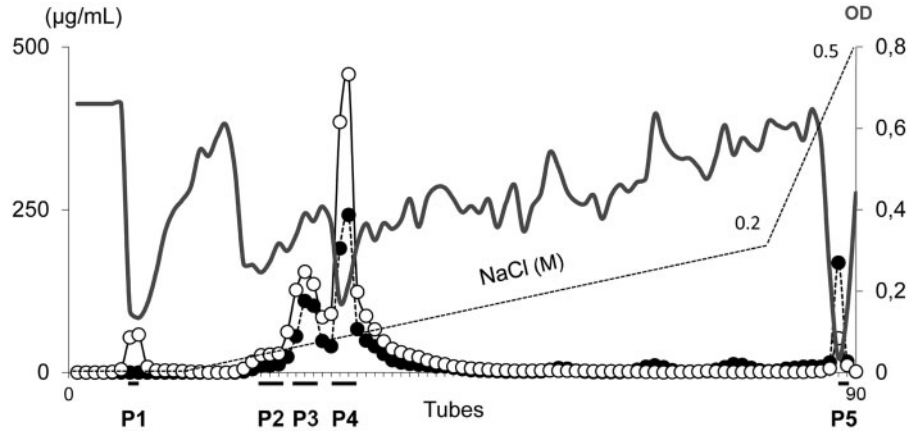

Fig. 3 Epitope detection anion-exchange chromatography of RUP oligosaccharides. The RUP oligosaccharides were fractionated in an NaCl gradient (dotted line). The uronic acid (dotted line with filled circles) and neutral sugar (solid line with open circles) contents were measured for each fraction and the binding of Sup2/INRA-AGI-1 to the fractions was tested in competitive inhibition ELISAs where the antigen coated on the ELISA plates was RUP–BSA. To visualize pools of interest, the OD obtained from the test of inhibition (solid line) was overlapped with the elution profile of RUP oligosaccharides. The binding of Sup2/INRA-AGI-1 was strongly inhibited in five pools annotated in the figure from P1 to P5.

Table 1 Glycosidic linkage analysis of RUP oligosaccharides and related anion-exchange chromatography-resolved pools P1–P4

Linkages	P1		P2		P3		P4	
	% Total sugar	Repartition per individual sugar	%mol Total	Repartition per individual sugar	%mol Total	Repartition per individual sugar	%mol Total	Repartition per individual sugar
t-Rha	0	0	0	0	0.4	1.1	2.4	7.3
2-Rha	0	0	0	0	0	0	5.3	15.8
4-Rha	0	0	9.1	40.1	15.6	46.5	7.8	23.3
2,4-Rha	0	0	11.8	52.3	17.2	51.2	17.4	51.8
2,3,4-Rha	0	0	1.7	7.6	0.4	1.2	0.6	1.7
Total	0	0	22.6	100	33.7	100	33.6	100
t-Ara*p*	0	0	1.8	6.6	2.8	9.7	6	24.7
t-Ara*f*	0	0	8	29.4	11.5	40.1	5.6	22.7
5-Ara	40.1	100	17.4	64	13.9	48.1	12.1	49.7
3,5-Ara	0	0	0	0	0.6	2.1	0.7	2.9
Total	40.1	100	27.2	100	28.8	100	24.4	100
t-Gal	21.4	35	22.8	47.3	33.1	88	29	70.9
3-Gal	0	0	1.7	3.6	1.8	4.8	1.6	3.9
6-Gal	0	0	2.7	5.5	0.3	0.7	1.6	4.1
4-Gal	38.5	65	17.1	35.4	1.9	5.3	8.1	20
3,4-Gal	0	0	2.4	4.9	0.2	0.5	0.1	0.4
4,6-Gal	0	0	1.6	3.3	0.3	0.8	0.3	0.7
Total	59.9	100	48.2	100	37.6	100	40.8	100
t-Xyl	0	0	2	100	0	0	0.8	100
Total	0	0	2	100	0	0	0.8	100
t-Glc	0	0	0	0	0	0	0.4	50
Total	0	0	0	0	0	0	0.4	50

Values are expressed as mole percentages of the total neutral sugar derivatives identified.
p, pyranose; *f*, furanose

were identified based on GalA and neutral sugar content and the EDC results. P1, P2 and P5 represented a very low proportion of the total RUP oligosaccharides. Nonetheless, P1, which contained exclusively neutral sugars, P5 which comprised a high proportion of GalA, and, to a lesser extent, P2, which contained both acid and neutral sugars, were particularly well recognized by the antibody. In contrast, P3 and P4 were poorly recognized by the new mAb, considering that they represent the most abundant portion of the total RUP oligosaccharides.

Linkage analysis was performed on pools P1–P4 (**Table 1**). P5 could not be analyzed as the amount of neutral sugars it contained was insufficient. P1 was composed solely of Ara*f* and

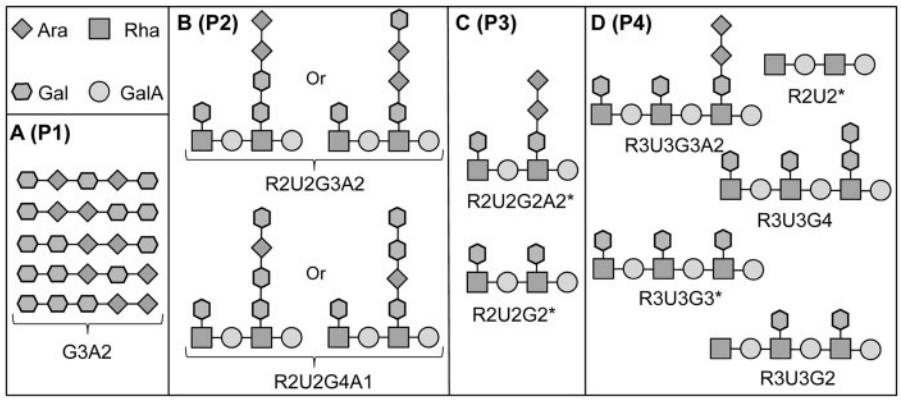

Fig. 4 Oligosaccharides contained in the pool P1 (a); P2 (b), P3 (c) and P4 (d). (A, B) were deduced from the glycosidic linkage analysis; (C, D) were identified by mass spectrometry. P1, strongly recognized by Sup2/INRA-AGI-1, mostly contained DP 5 oligomers made of three Gal and two Ara residues connected together. The different fragments possibly present in P1 are shown in (A).

Gal*p* (**Table 1**). This pool that is strongly recognized by Sup2 (**Fig. 3**) thereby encompasses free RGI side chains, not attached to an RU backbone. Surprisingly, solely 5-linked Ara*f* units and no t-Ara*f* or t-Ara*p* units were detected. Galactose was present as 4-linked and terminal units. Since neither branching points nor terminal Ara units were detected, 5-linked arabinan stretches will be included into a 4-linked galactan chain. Considering the proportion of 5-linked Ara*f*, 4-linked Gal*p* and t-Gal*p*, the following overall structure can be proposed:

$$[(1\rightarrow4)\text{-}\beta\text{-D-Gal}p]_x\text{-}[(1\rightarrow5)\text{—}\alpha\text{—L-Ara}f]_y\text{-}[(1\rightarrow4)\text{-}\beta\text{-D-Gal}p]_z$$

RUP oligosaccharides were obtained after enzymatic treatment of the purified potato RGI polymer by endogalactanase and endoarabinanase, and, since t-Gal is present in large amounts, it is unlikely that x, y and z exceed a value of 3.

P2, P3 and P4 were similar with respect to Rha/Ara/Gal ratios. In P2 and P3, an RU backbone DP of 4 can be calculated and a vast majority (99–100 mol%) of the Rha*p* units appear branched at *O*-4. In contrast, close to 25% of the Rha*p* units present in pool P4 were unbranched (terminal and 2-linked) and an average DP of 6 could be calculated for the RU backbone. The average length of side chains also differed significantly between P2, P3 and P4. P2 contained a higher proportion of internal Gal units (mainly 4-linked Gal*p*) and internal 5-linked Ara*f* units than P3 and P4, which contained mainly t-Gal*p* but also t-Ara*f*. Ara- and Gal-containing side chains were shorter in P3 (average DP1.5) and P4 (average DP1.6) compared with P2 (average DP2.5).

The two main pools (P3 and P4) recovered by anion-exchange chromatography were further analyzed by LC-MS (**Supplementary Fig. S1**). From linkage analysis, it was hypothesized that P3 and P4 were mainly composed of oligosaccharides with a DP4 and DP6 RU backbone, respectively, that were highly branched at *O*-4 of Rha units, mainly by single Gal*p* residues. In agreement with linkage analysis results, the major compounds identified in P3 and P4 were $R_2U_2G_2$ (*m*/*z* 985) and R3U3G3 (*m*/*z* 734, doubly charged), respectively (**Supplementary Fig. S1**). Interestingly, only two oligosaccharides were detected in P3: $R_2U_2G_2$ and $R_2U^2G_2A_2$. Since Sup2 did not bind to $R_2U_2G_2$, it is likely that $R_2U_2G_2A_2$ is the oligosaccharide recognized in P3. Fragmentation of $R_2U_2G_2A_2$ by tandem mass spectrometry (MS/MS) showed that this molecule is not symmetrical (**Supplementary Fig. S2**). Indeed, the ion C_2 at *m*/*z* 501.2 corresponds to a fragment containing one Rha, one GalA and one Gal unit, whereas the Z_2 ion at *m*/*z* 747.3 contains, in addition to the same three sugars, the two Ara residues. The detection of a $^{2,4}A_4$ ion at *m*/*z* 1115.3 provides evidence that the reducing end of the molecule consists of GalA. The Z_3 ion at *m*/*z* 923.3 has lost a fragment containing one Rha and one Gal at the non-reducing end of the molecule. These results show that the two Ara residues and one Gal residue are branched onto the internal Rha residue next to the reducing GalA unit. The Gal and Ara residues could be included in a single side chain or in two distinct chains branched at *O*-3 and *O*-4 of the Rha residue. The presence of the ion generated from an intracyclic fragmentation at *m*/*z* 543.2 ($^{1,3}A_3$) provides evidence that the internal Rha*p* unit is not branched at *O*-3. This ion corresponds to a trimer of Gal, Rha and GalA carrying a fragment of the internal Rha*p* residue containing C-2 and C-3 (**Supplementary Fig. S2B**). Therefore, the internal Rha unit is solely branched at *O*-4 with a trimeric chain encompassing one Gal and two Ara residues. The two Ara residues are likely to be branched as a dimer on the Gal unit since the two pentose units were systematically released together after fragmentation. Indeed, the ion assigned to Z_3, having lost the two Ara units, was detected at *m*/*z* 659.3. Similarly, the two ions at *m*/*z* 599.3 (Z_3-$^{1,3}A_3$-2Ara) and *m*/*z* 581.2 (Z_3-$^{1,3}A_3$-H_2O-2Ara) do not contain the pentose dimer. However, from the fragmentation pattern, it is not possible to determine the nature of the link between the Gal residue and Ara dimer.

Similarly, the oligosaccharide at *m*/*z* 866.2 present in P4 was assigned to a DP6 RU backbone with one unbranched Rha, one Rha branched by a single Gal residue and one Rha branched by a Gal residue substituted by an Ara dimer (not shown).

To conclude, sugar linkage and mass spectrometry analyses evidenced the presence of a structure encompassing 5-linked Ara and 4-linked Gal included in a single linear chain in the pools P1–P4 (**Fig. 4**). Since the supernatant binds to a type I arabinogalactan motif, the new antibody was named INRA-AGI-1.

INRA-AGI-1 binding to cell walls of potato tuber and carrot root is increased by a pre-treatment with galactanase

The capacity of the INRA-AGI-1 antibodies to bind pectin in situ was studied using transverse sections of the peripheral region of potato tuber (Fig. 5A). The labeling pattern of the INRA-AGI-1 antibodies was compared with that of available RGI-related antibodies (LM5, LM6 and INRA-RU1). No labeling was observed with INRA-AGI-1 in the absence of enzymatic pre-treatment of the section (Fig. 5C, E). Cell walls of the cortex were strongly labeled with LM5 (Fig. 5I) and the labeling showed a gradient of the epitope abundance across the periderm and outer cortex (Fig. 5G) as described in other studies (Bush and McCann 1999, Bush et al. 2001, Sabba and Lulai 2004). The walls from periderm and cortex were labeled moderately with LM6 (Fig. 5K–M) and no clear gradient was observed along the transverse sections. INRA-RU1 bound the potato walls of the periderm and cortex region, with a stronger labeling in the outer region (Fig. 5O) than the inner region of the tuber (Fig. 5Q).

As long galactan side chains may impede the access of antibodies other than LM5 to their epitopes, sections were treated with endogalactanase prior to the immunolabeling procedure. The decrease of labeling with LM5 after galactanase pre-treatment confirmed the efficiency of galactan digestion (Fig. 5H–J). The degradation of galactan led to the detection of the INRA-AGI-1 epitope across the section (Fig. 5B). The epitope was more abundant in the periderm and outer cortex (Fig. 5B–D) than in the inner cortex (Fig. 5F). The labeling with LM6 and INRA-RU1 was also increased after galactanase pre-treatment (Fig. 5L–N, P–R). To investigate further the impact of RGI traits in the INRA-AGI-1 binding in situ, sections pre-treated with galactanase were incubated with an endoarabinanase alone or sequentially with an arabinanase and a rhamnogalacturonan hydrolase, or an arabinanase and a pectin lyase, prior to immunolabeling (Supplementary Fig. S3). The binding of INRA-AGI-1 was slightly enhanced with the double treatment involving the galactanase and the arabinanase (Supplementary Fig. S3B). Further enzymatic deconstruction involving rhamnogalacturonan hydrolase increased the epitope detection (Supplementary Fig. S3C), but no difference in the pattern of epitope occurrence was revealed. Removal of HG by pectin lyase after the galactanase and arabinanase treatments did not improve the detection of the INRA-AGI-1 epitope (Supplementary Fig. S3D). When the pectin lyase was used on its own to pre-treat the sections, no labeling was observed, even in the middle lamella (not shown). As none of the enzymatic treatments resulted in loss of the INRA-AGI-1 epitope, it could be concluded that the epitope is recalcitrant to available RGI and HG enzyme actions.

The occurrence of the RGI-related epitope in the outer cortex was investigated at the ultrastructural level. As seen by light microscopy, in sections in which galactan had not been enzymatically removed, INRA-AGI-1 epitope was not detected (Fig. 6A). After removal of galactan, the INRA-AGI-1 epitope was detected throughout most cell walls (Fig. 6B) and also at cell junctions (Fig. 6D). The expanded middle lamella at filled intercellular spaces was also labeled (Fig. 6D). In the absence of galactanase pre-treatment, INRA-RU1 binding was concentrated in the middle lamellae (Fig. 6E, F). Removal of galactan led to detection of the INRA-RU1 epitope throughout the wall (Fig. 6G, H) except in the inner region very close to the plasma membrane and at filled intercellular spaces (Fig. 6I). The LM6 epitope in the absence of pre-treatment with galactanase was detected throughout the wall except in the region of expanded middle lamella at cell corners (Fig. 6I–M). The LM5 epitope was mostly restricted to the primary walls (Fig. 6J, K) as previously described (Bush and McCann 1999).

In conclusion, the distribution pattern of the INRA-AGI-1 epitope differs from patterns described for pectic epitopes to date. It was unmasked by the removal of galactan, but did not co-localize with the LM5 epitope. The INRA-AGI-1 epitope only partially co-localized with LM6 and INRA-RU1 epitopes.

The occurrence of the INRA-AGI-1 epitope was also determined in carrot root cell walls where a galactanase pre-treatment was essential for its detection. The labeling was very faint and, when present, restricted to the middle lamellae (Fig. 7A), lining intercellular spaces (Fig. 7B) or at filled spaces (Fig.7C). As observed in potato tubers, the INRA-AG1 epitope did not co-localize with LM5 (Fig. 7G–I) and only partly with the INRA-RU1 epitope (Fig. 7D–F).

Immunolabeling results on both potato tuber and carrot root sections confirmed the occurrence of the epitope in middle lamellae. However, the notable difference was that in addition to middle lamella, the epitope was also detected in the primary cell walls of potato tubers.

Discussion

Occurrence of internal arabinose in type I arabinogalactan from potato tuber RGI extract

RUP oligosaccharides were purified from raw RGI solubilized from potato pulp by alkaline extraction. Using a combination of RGI enzymes to degrade the side chains and split the RGI backbone, we have succeeded in recovering low DP RGI oligosaccharides highly branched with short side chains. Most of the oligosaccharides contained only Gal side chains. Similar oligosaccharides arising from a rhamnogalacturonan hydrolase digest of 'modified hairy regions' were identified in apple (Colquhoun et al. 1990), carrot, onion, leek, potato, pear (Schols et al. 1994, Schols and Voragen 1994) and sugar beet (Ralet et al. 2010). In our study, oligosaccharides containing both Ara and Gal were additionally identified ($R_2U_2G_2A_2$, $R_3U_3G_2A_1$ and $R_3U_3G_3A_2$) but no α-L-arabinose directly branched onto Rha*p* was detected. Interestingly, fragmentation of $R_2U_2G_2A_2$ by MS/MS revealed that the two Ara units were linked as a dimer to one Gal unit attached to the internal Rha residue. These results strongly suggest that arabinan side chains are branched to the RGI backbone through a Gal moiety. As a matter of fact, only a few studies have reported a direct connection of arabinan side chains to the RGI backbone (Lau et al. 1987, Ducasse et al. 2011).

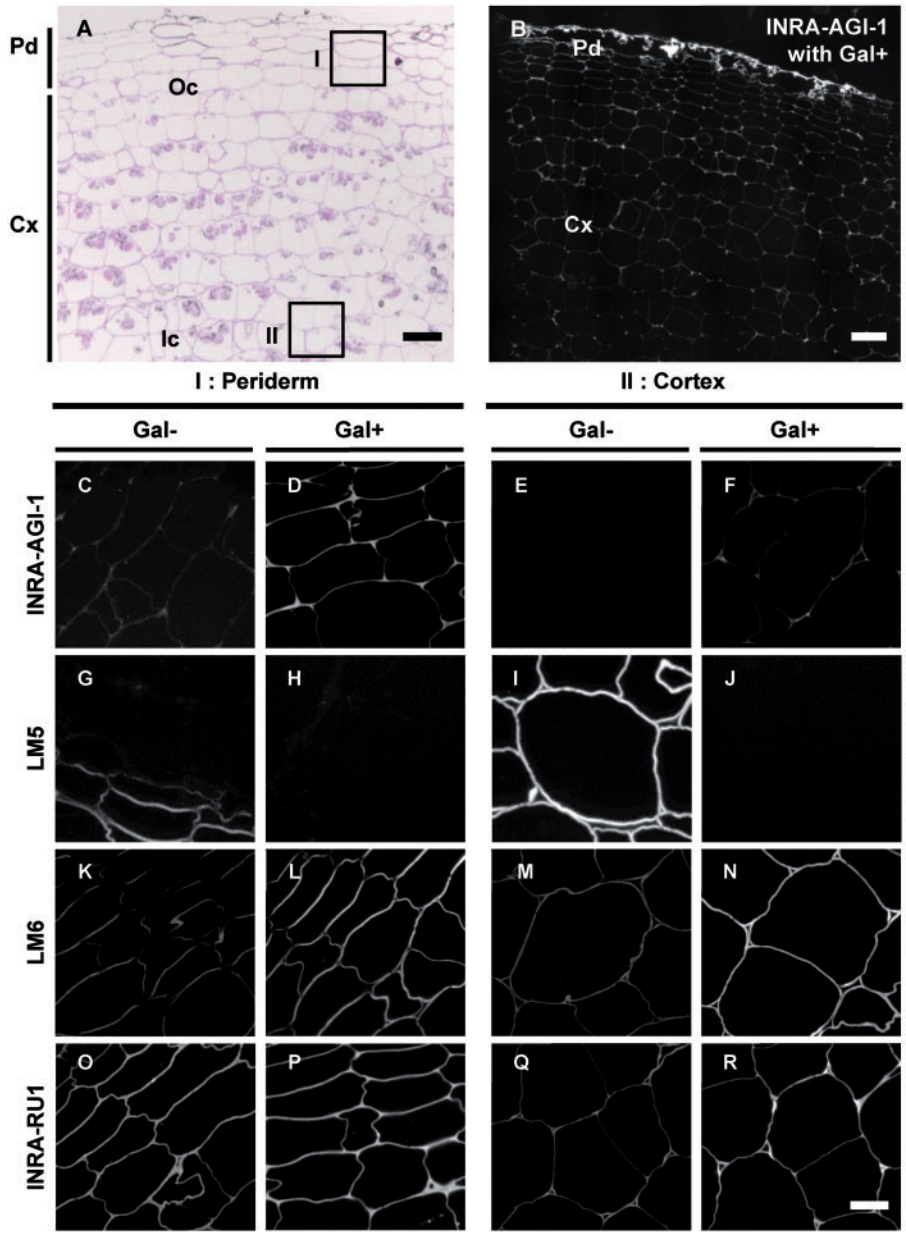

Fig. 5 Immunofluorescence labeling of periderm and cortical tissues of potato tubers by INRA-AG-1, LM5, LM6 and INRA-RU1. (A) Transverse cross-section of a potato tuber stained with toluidine blue shows the different tissue types. I corresponds to the peridermal area where the representative images (C, D, G, H, K, L, O and P) were acquired. II is the cortical region where (E, F, I, J, M, N, Q and R) were captured. (B) Representative transverse cross-section of a potato tuber pre-reated with an endogalactanase (Gal+) and immunolabeled with INRA-AGI-1. (C, E, G, I, K, M, O and Q) The immunolabeling of sections that were not subjected to enzymatic pre-treatment (Gal−). (D, F, H, J, L, N, P and R) The immunolabeling of sections pre-treated with an endogalactanase (Gal+). Representative micrographs of peridermal and cortical cells immunolabeled with INRA-AGI-1, LM5, LM6 and INRA-RU1 are shown from C to F, G to J, K to N and O to R, respectively. The deconstruction of galactan was a prerequisite to detect the INRA-AGI-1 epitope (B–F). The binding of INRA-AGI-1 appears as a radial gradient in the transverse section with a high level of detection in the external layers that decreases in abundance towards the inner layers of cells (B, D and F). A similar gradient was observed with INRA-RU1 (O, Q), whereas the detection of the LM5 epitope (G and I) showed a reverse gradient of abundance when compared with INRA-AGI-1. No clear gradient of detection along the transverse section was observed for the LM6 epitope (K, M). The LM5 detection was lost after endogalactanase pre-treatment (H and J). In contrast, the endogalactanase pre-treatment leads to an increase of detection of the LM6 (L and N) and INRA-RU1 (P and R) epitopes. Pd, periderm; Cx, cortex; Oc, outer cortex; Ic, inner cortex. Scale bar = 100 μm (A, B); 50 μm (C–R).

In a previous study, the structural complexity of potato RGI side chains was highlighted (Øbro et al. 2009). Indeed, Øbro and co-workers have shown that β-(1→4)-galactans were released by endoarabinanase treatment of purified potato RGI. Furthermore, Ara was released by endogalactanase treatment of the same substrate. The authors have suggested that (i) β-(1→4)-galactans may carry few substitutions of short arabinan chains; (ii) α-(1→5)-arabinans may be attached to the RGI

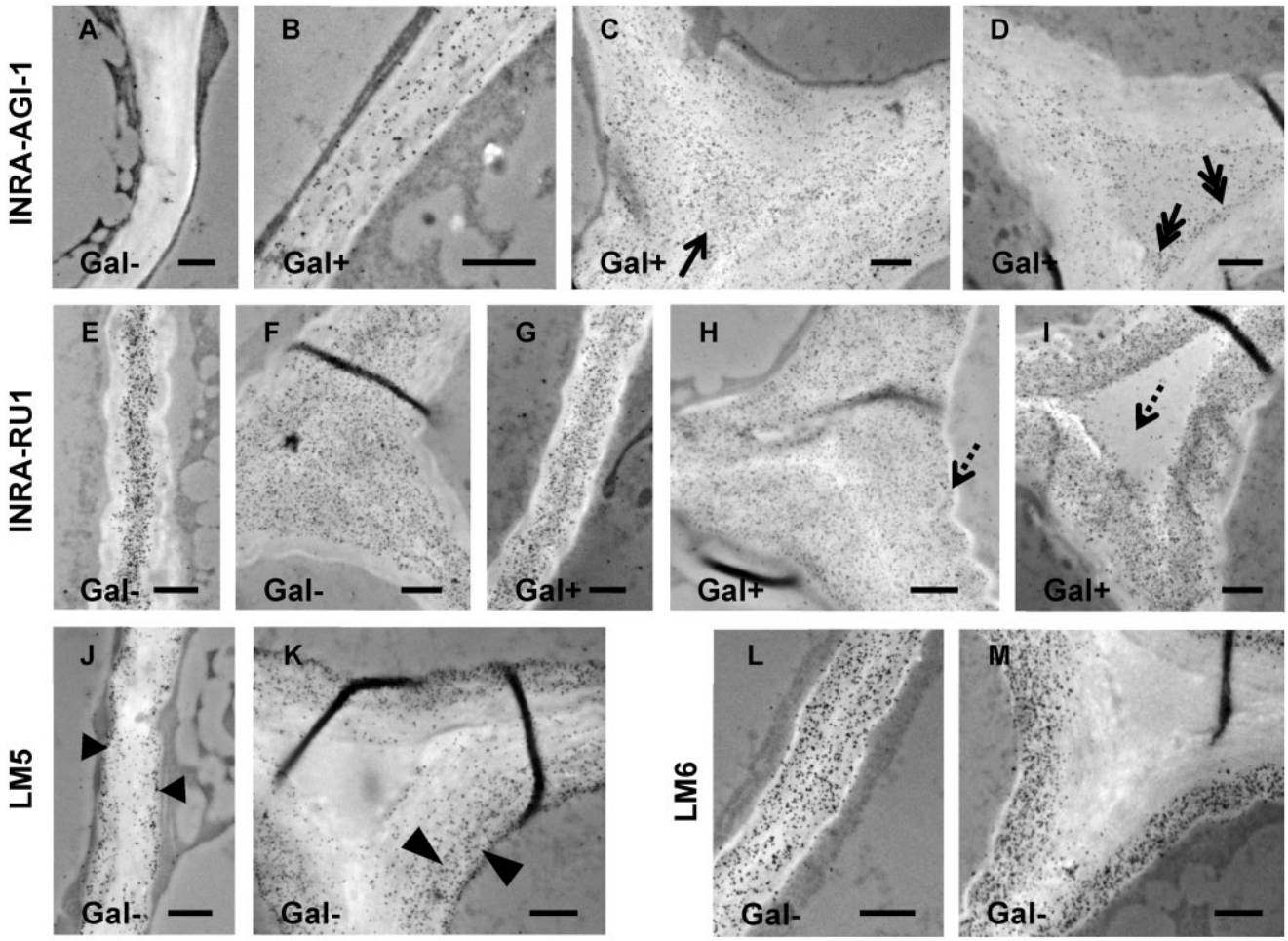

Fig. 6 Immunogold labeling of potato tuber cell walls with INRA-AGI-1 (A–D), INRA-RU1 (E–I), LM5 (J–K) and LM6 (L–M). Sections in B–D and F–I were pre-treated with endogalactanase prior to immunolabeling (Gal+). The INRA-AGI-1 epitope is unmasked by removal of galactan (A–D). It is distributed throughout the wall [as shown in a low magnication micrograph (B) including the middle lamella (as highlighted by the arrow in C)] and filled corners (highlighted by double-headed arrows in D). In the absence of endogalactanase pre-treatment (Gal–), unbranched RGI backbone, recognized by INRA-RU1, is only marked in the middle lamella (E, F) whereas it is detected in both the middle lamella and primary cell walls after the degradation of galactan (G–I). The dashed arrows in (H) and (I) highlight the absence of INRA-RU1 detection in the inner wall region close to the plasmalemma and filled cell corners, respectively. The LM5 epitope is mainly localized at the primary walls (as indicated by the arrowheads in J and K) whereas the LM6 (L–M) epitope is readily detected throughout the wall except at cell corners where the middle lamella expands. Scale bar = 1 μm.

backbone through short galactan anchor chains; and (iii) β-(1→4)-galactans may be present as side chains or extensions of arabinans. Type I arabinogalactans containing both Ara and Gal residues linked in a linear chain have not been frequently reported. This structure was evidenced in CDTA-extractable soybean pectin on which free oligosaccharides made of (1→4)-linked Gal interspersed with one internal (1→5)-linked Ara*f* were identified (Huisman et al. 2001). Interestingly, in the present study, a similar structure was identified in the neutral pool (P1) of the RUP oligosaccharides. Complex Ara- and Gal-containing side chains have also been found in other RGI-rich extracts. In suspension-cultured sycamore cells, Ara*f* was found linked to *O*-3 of Gal branched at *O*-4 of Rha (Lau et al. 1987). In *Gossypium hirsutum* L., Zheng and Mort (2008) have also isolated the $R_2U_2G_2A_2$ fragment. in contrast to our findings, the two Ara units were not linked together but branched onto a Gal residue as single units, one at the *O*-3 position and one at the *O*-4 position.

INRA-AGI-1 recognizes a type 1 arabinogalactan motif

mAbs were raised against the RUP oligosaccharides and one of them (INRA-AGI-1) was characterized in detail. A high-throughput screening of its antigenicity recognition using glycan microarrays has shown that INRA-AGI-1 has a novel binding pattern compared with the available RGI-related mAbs. INRA-AGI-1 appeared to be very specific. It did bind to potato and soybean polymeric RGI and to RUP oligosaccharides, and competitive inhibition ELISAs have provided evidence that the epitope was also present in two other cell wall pectic galactan-rich plant sources, carrot and lupin. However, INRA-AGI-1 did not react with any of the other polymeric and

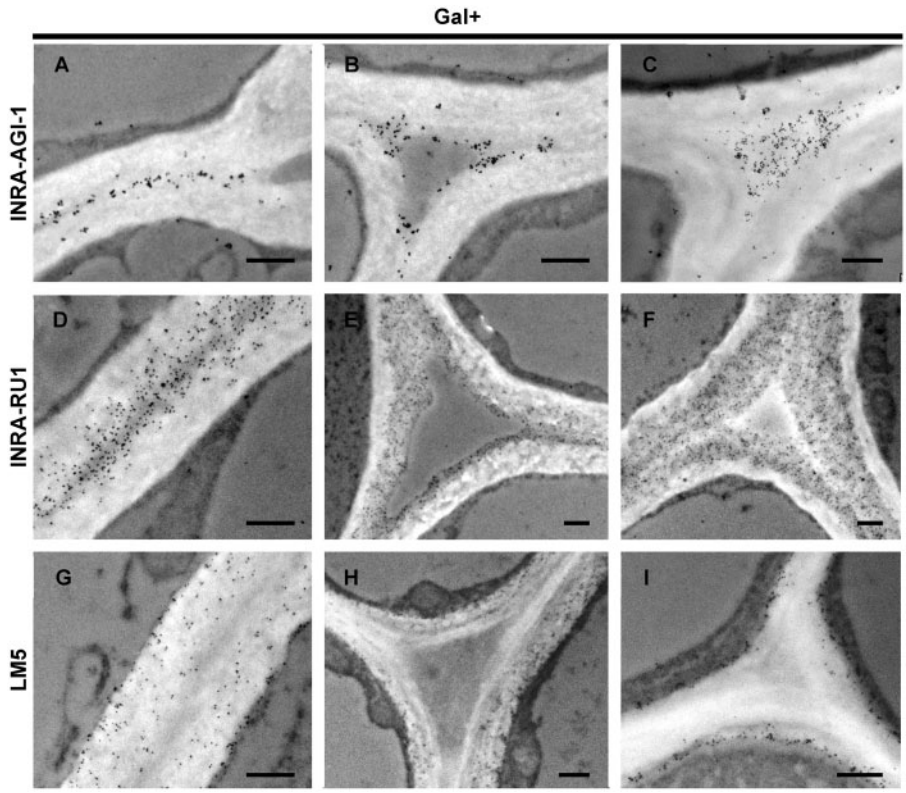

Fig. 7 Immunogold labeling of carrot root cell walls with INRA-AGI-1 (A–C), INRA-RU1 (D–F) and LM5 (G–I). All sections were pre-treated with endogalactanase prior to immunolabeling. Labeling with INRA-AGI-1 is restricted to the middle lamella (A) including the filled cell corners (B, C). The INRA-RU1 epitope is mainly localized at the middle lamella and in the primary wall region adjacent to the middle lamella (D–F). INRA-RU1 does not bind to filled corners (F). The LM5 epitope is localized in the inner region of the primary wall (G–I). Scale bar = 0.5 μm.

oligomeric pectin-related substrates tested; notably, HG, AGII and oligosaccharides arising from (1→4)-linked galactan, (1→5)-linked arabinan, unbranched RGI backbone and branched RGI backbone by single Gal residues ($R_2U_2G_2$) were not recognized.

In order to obtain further insight into the epitope structure, a variant to the epitope detection chromatography technique developed by Cornuault et al. (2014) was implemented. RUP2 antibody bound a minor neutral fraction (P1) containing oligosaccharides of (1→4)-linked Gal*p* residues interspersed with internal (1→5)-linked Ara*f* residues, indicating that the RGI backbone is excluded from the epitope recognition. Interestingly, two other anion-exchange chromatography-resolved fractions (P3, P4) which, to a lower extent, also reacted with INRA-AGI-1 contained RGI backbone fragments branched with Ara and Gal linked in the same chain ($R_2U_2G_2A_2$ and $R_3U_3G_3A_2$). Taken altogether, our results suggest that the epitope recognized by INRA-AGI-1 antibodies is a linear structure, which consists of:

$$[(1\rightarrow4)\text{-}\beta\text{-D-Gal}p]_x\text{-}[(1\rightarrow5)\text{—}\alpha\text{—L-Ara}f]_y\text{-}[(1\rightarrow4)\text{-}\beta\text{-D-Gal}p]_z$$

with x, y and z values ranging from1 to 3.

The presence of (1→4)-linked Gal residues in the epitope and the fact that the antibody showed a strong specificity for the RGI extract and no binding to the majority of the other cell wall extracts we have tested by glycan microarrays are in favor of an RGI origin for this motif. However, it cannot be precluded that this peculiar motif might be a linkage or anchor domain that tethers different glycans together. Indeed, in addition to RGI 'internal' structural complexity, there is increasing evidence that RGI could be part of glycan mega-structures encompassing several cell wall polymers. An arabinoxylan–pectin–arabinogalactan protein complex (APA1) has recently been isolated from Arabidopsis suspension culture media (Tan et al. 2013). Interestingly, two antibodies to heteroxylan were produced using RUP oligosaccharides as immunogens (Cornuault et al. 2015).

Occurrence of RGI-related epitopes in potato tuber cell walls

The INRA-AGI-1 epitope was detected in situ in potato tuber and carrot root cell walls, but enzymatic removal of galactan was a prerequisite. If we assume that the epitope in planta is attached on the RU backbone, it could be hypothesized that it is at least partly present close to the backbone. Indeed, if the short internal (1→5)-linked Ara units would have only been present far from the RU backbone (i.e. a long galactan chain anchor to the RU backbone), the galactan anchor would have been hydrolyzed by endogalactanase and the epitope would have been lost. INRA-AGI-1 binding was shown to increase slightly after arabinan and RGI backbone enzymatic hydrolysis.

It is noteworthy that total depletion of potato RGI side chains by extensive arabinan- and galactan-degrading enzymes cannot be achieved (Sørensen et al. 2000, Skjøt et al. 2002, ØBro et al. 2009, Larsen et al. 2011).

Altogether, these observations suggest that the presence of the INRA-AGI-1 epitope is masked by long galactan side chains and that the epitope is partially protected from the action of RGI hydrolases.

An increasing gradient of INRA-AGI-1 epitope abundance towards the outer cortex was observed.

The detection of the INRA-RU1 and LM6 epitopes increased after galactanase treatment, confirming that these epitopes are partially masked by galactan present in large amounts in potato tuber. No gradient of LM6 and INRA-RU1 epitopes was revealed after galactanase treatment.

At the ultrastructural level, the INRA-AG-1 epitope did not co-localize strictly with any of the known RGI epitopes. It was found to be present in primary cell walls and middle lamellae in potato tuber. In carrot roots, it was restricted to middle lamellae. The INRA-AGI-1 epitope is therefore a novel, previously unidentified, epitope, and its presence or extent of masking may be regulated at both the level of tissues and across cell walls.

In the last 15 years, notable differences in the distribution of RGI epitopes in relation to cell type and developmental stage in different organs have been revealed by immunohistochemistry (Willats et al. 1999, Ermel et al. 2000, Bush et al. 2001, McCartney et al. 2003). The arabinan LM6 epitope has been predominantly detected in proliferating cells while the galactan LM5 epitope has been observed in elongating cells and cambium. However, the appearance of galactan is not always correlated with cell elongation. In pea cotyledon cell walls, galactan appears quite late in development while arabinan is present throughout development (McCartney et al. 2000). In mature potato tubers, galactan is the major cell wall polysaccharide (Jarvis et al. 1981). In this study, we clearly showed that RGI epitopes are also not evenly distributed throughout the wall at the cell level. This confirms previous results obtained with the set of antibodies that was available at the time (Bush and McCann 1999, Bush et al. 2001, Lee et al. 2013). The restricted location of the galactan LM5 epitope to the inner region of the wall while galactan accounts for the major cell wall polysaccharides in potato raises a question about the representativeness of the LM5 epitope for galactan and arabinogalactan. The occurrence of some forms of galactan-containing elements that are not accessed by LM5 is suggested by the treatments with endogalactanase that result in unmasking of the INRA-AGI-1 epitope in cell wall regions where the LM5 epitope is not detected. Non-strict co-localization of RGI epitopes at the cell wall level strongly suggests that different populations of RGI molecules may be synthesized at different times during cell wall development and may co-exist in muro: RGI with a low density of side chains in the middle lamella, and galactan- or arabinan-rich RGI in the primary wall. The existence of distinct populations of RGI side chains is supported by the analysis of Arabidopsis mutants that lack pectic arabinan or galactan synthase activity. Indeed, the inactivation of GALS1, a galactan galactosyltransferase (Liwanag et al. 2012), and ARAD1, a putative arabinan arabinosyltransferase (Harholt et al. 2006, Harholt et al. 2012), led to a partial reduction of galactan and arabinan, respectively, and both enzyme activities have been shown to be developmentally regulated. It can therefore be expected that several enzymes are required for the RGI side chain biosynthesis—probably regulated during wall formation—which would therefore result in distinct RGI subpopulations. This is reflected in the observations presented here. The heterogeneity of RGI revealed by epitope detection anion-exchange chromatography applied on alkaline cell wall extracts of tobacco seed endosperm also supports the co-existence of different RGI populations (Lee et al. 2013). Possibly not all side chains are attached to the RGI backbone. Neutral arabinan and galactan free of GalA and Rha have been isolated from mung bean hypocotyls (Herve du Penhoat et al. 1987). Data obtained from transgenic potato plants (Oomen et al. 2002) are, however, against this hypothesis. Transgenic potato plants expressing a rhamnogalacturonan lyase produce tubers with altered morphology and reduced amounts of both Gal and Ara (Oomen et al. 2002). The remaining galactan is found in the middle lamella at cell corners which is in contrast to its location in the primary walls of wild-type tubers. This suggests that anchoring of galactan and arabinan to the RGI backbone is required at least for correct insertion into cell walls.

As the set of available mAbs to RGI increases, it appears that RGI side chains are more diverse than initially thought, with complex patterns of occurrence at both the tissue and cell wall levels. INRA-AGI-1 is the second antibody, with LM16, which recognizes a motif involving both Gal and Ara residues. Both antibodies recognize distinct patterns, as LM16 is proposed to bind to a terminal Gal residue after arabinanase treatment (Verhertbruggen et al. 2009a) and INRA-AGI-1 recognizes a short stretch of arabinan surrounded by Gal residues. Interestingly, the epitope detection of both antibodies is increased following enzymatic degradation. The biosynthesis and remodeling of pectin in plant cell walls is poorly understood and, here, we present a new mAb available to the plant community that should contribute to understanding such mechanisms further.

Materials and Methods

Plant material, enzymes and glycans

Plant material. Potato pulp (Ref: 74739; 2003) was provided by Roquette (Lestrem, France). Carrot roots were kindly gifted by Guy Chevalier.

Enzymes. The purified endo-1,4 -β-galactanase (940 UI ml^{-1}; from *Aspergillus niger*) was obtained from Megazyme. Endo-1,5-α-arabinanase (950 UI ml^{-1}, from *A. niger*) was prepared as previously reported (Bonnin et al. 2002). Rhamnogalacturonan hydrolase from *Aspergillus aculeatus* (Batch PPJ4478) was purchased from Novozyme. Pectin lyase (57.6 nkat ml^{-1}) was purified in the laboratory from a crude preparation Peclyve of *A. niger* (Lyven) following the method described in Ralet et al. (2012).

Glycans. Polysaccharides used in the present work are referenced in **Table 2**. RGI backbone oligosaccharides (R_nU_n oligosaccharides with $n = 2–18$, designated RU oligosaccharides; R, Rha and U, GalA,) were isolated

Table 2 Sources and sugar composition of polysaccharides used for the characterization of mAbs

Glycans	Sources	Sugar composition (molar % of the total sugars)
Sugar beet pectin (SBP6230)	Ralet et al. (2003)	Rha, 6.4; Ara, 14.9; Gal, 12.6; GalA, 66.2
Lemon pectin	Danisco	ND
Apple pectin	Danisco	ND
Lime pectin DM: 81% (E81)	Ralet et al. (2001)	Rha, 1.5; Ara, 0.3; Gal, 4.7; GalA, 93.5
Lime pectin DM: 15% (B15)	Ralet et al. (2001)	Rha, 0.9; Ara, 0.2; Gal, 1.8; GalA, 97.1
Lime pectin DM: 34% (B34)	Ralet et al. (2001)	Rha, 0.9; Ara, 0.2; Gal,1.8; GalA, 97.1
HG citrus (DM 0)	Tanhatan-Nasseri et al. (2011)	GalA >98%
RGI soybean	Megazyme	Rha, 13; Ara, 3.5; Gal,12.5; GalA, 51; Fuc, 10; Xyl, 13.7
RGI beetroot	INRA-Nantes	Rha, 7; Ara, 47; Gal, 10; GalA, 36
RGI carrot	INRA-Nantes	Rha, 5.3; Ara, 6; Gal, 23.1; GalA, 62.5
AG II (Larch wood)	Sigma	ND
AGP (Larch wood)	Megazyme	Purity >5% (Ara, 15; Gal, 85)
Potato pectic galactan	Megazyme	Rha, 3; Ara, 6; Gal, 82; GalA, 9
Potato galactan A	Megazyme	Rha, 3; Ara, 2; Gal, 88; GalA, 7
Potato galactan B	Lahaye et al. (1991)	Rha, 0.2; Ara, 1.6; Gal, 86.4; GalA, 1.4
Lupin galactan	Megazyme	Rha, 4.2; Ara, 20.9; Gal, 71.3; GalA, 5
Branched arabinan (sugar beet)	Megazyme	Rha, 2; Ara, 88; Gal, 3; GalA, 7
Linear arabinan (sugar beet)	Megazyme	Ara, 97.5; Gal, 0.4; Rha, 0.1; GalA, 2

ND, not determined.

from *Arabidopsis thaliana* seed mucilage by Ralet et al. (2010). DP-resolved RU [designated RxUy(Gz), arabinan (DP5–12) and galactan (DP4–15)] oligosaccharides were prepared according to Ralet et al. (2010).

RUP oligosaccharides were generated from de-starched potato pulp. Potato pulp (10 g) was enzymatically de-starched (Cornuault et al. 2015) and the resulting suspension was mixed with NaOH (0.1 M final) and left for 2 h at 90°C. After filtration and neutralization, the filtrate was concentrated to 1.5 liters by rotary vacuum evaporation at 40°C. The extracted polymers were then precipitated with 2 vols. of ethanol overnight at 4°C. After centrifugation (8,100×*g*, 15 min), the supernatant was discarded and the pellet was re-suspended in an ethanol : water mixture (72 : 28, v/v) and centrifuged as described above. The pellet was then dissolved in distilled water and dialyzed to remove residual salts. Finally, the salt-free solution was filtered on a membrane (3 µm pore size) and freeze-dried. The so-called raw RGI fraction (1,200 mg; molar ratio Rha : Gal : GalA, 1 : 8.4 : 8.2) was further purified using DEAE-Sepharose fast flow gel. After pre-equilibration of the gel (150 ml) with 20 mM sodium acetate pH 4.5, raw RGI solution (400 mg in 40 ml of H_2O) was mixed with the gel and left for 20 min at room temperature with occasional manual stirring. The supernatant was recovered and the gel was further washed four times with 100 ml of 20 mM sodium acetate buffer pH 4.5. The supernatant and washes, that corresponded to an RGI-enriched fraction, were pooled and filtered on a G3 sintered glass. The whole procedure was performed three times and the three filtered RGI-enriched fractions were pooled, dialyzed and freeze-dried.

The RGI-enriched fraction (650 mg; molar ratio Rha : Gal : GalA, 1 : 12.7 : 2.6) was then dissolved in 50 mM sodium acetate buffer pH 4.5 (130 ml) and sequentially incubated with an endo-1,4-β-galactanase (from *A. niger*, Megazyme International, 1 ml, 2.35 U ml^{-1}) for 150 min at 40°C and an endo-1,5-α-arabinanase (cloned from *A. aculeatus* in *Aspergillus oryzae*, Novozyme, batch PPJ44381, 2.3 ml at 3.42 U ml^{-1}) for 24 h at 30°C to degrade galactan and arabinan side chains, respectively. The enzymes were inactivated by boiling the solution for 5 min and the released oligosaccharides were removed by dialysis. The galactan- and arabinan-depleted RGI fraction was freeze-dried.

The arabinan- and galactan-depleted RGI fraction (116 mg; molar ratio Rha : Gal : GalA, 1 : 1.3 : 1.7) was then incubated with GH 28 rhamnogalacturonan hydrolase (Novo Nordish Batch PPJ4478, 25 g of recovery pilot plant 09/12/1993, 300 µl at 1 mg ml^{-1}) in 10 mM sodium acetate pH5 for 180 min at 40°C to split the RGI backbone. Large fragments were removed by ethanolic precipitation (50%, overnight at 4°C) followed by centrifugation (10 min, 15,000×*g*). The ethanol-soluble fraction was recovered, concentrated by rotary vacuum evaporation, desalted and freeze-dried. This was designated as RUP oligosaccharides (78 mg).

Anion-exchange chromatography

Separation was performed at room temperature using a DEAE-Sepharose fast flow gel column (1.6×13.5 cm). The gel was equilibrated with degassed 25 mM Na acetate buffer pH 5.5 at a flow rate of 1 ml min^{-1}. RUP oligosaccharides (20 mg 2 ml^{-1}) were loaded onto the column. The gel was washed with 51.6 ml of 25 mM Na acetate buffer. The material attached to the column was eluted with a linear gradient of NaCl (0.025–0.2 M) in 25 mM Na acetate buffer (262 ml) and with 0.5 M NaCl in 25 mM Na acetate buffer (34 ml). RUP oligosaccharides were recovered in 90 tubes which were analyzed for their neutral sugar and galacturonic acid content.

Sugar analysis

Uronic acid and neutral sugar analyses. Uronic acid content was determined by the automated *m*-hydroxybiphenyl assay (Thibault 1979). The difference in response of glucuronic acid and GalA in the presence and absence of tetraborate was used to differentiate them (Renard et al. 1999). Total neutral sugars were quantified by orcinol assay with correction for the GalA acid interference (Tollier and Robin 1979). Individual neutral sugars were analyzed as their alditol acetates by gas–liquid chromatography (Englyst and Cummings 1988). Chromatography was performed on a fused-silica capillary column (30 m×0.32 mm) bound with OV-225 (50% cyanopropylphenyl dimethylpolysiloxane, temperature 210°C, carrier gas H_2). Inositol was used as internal standard and the assays were calibrated using a standard solution made of monomers.

Glycosidic linkage analyses of RUP oligosaccharides and derived anion-exchange chromatography fractions. RUP oligosaccharides and derived fractions solubilized in water (1 mg ml^{-1}) were converted into their H^+ form by percolating the solutions through a 1 ml Sigma Dowex ® 50WX4 resin. Once collected, the samples were freeze-dried and then dried in a vacuum oven at 40°C for 2 h before being dissolved in dimethylsulfoxide (DMSO; 0.2 ml) and sonicated for 2 min. The mixtures were left for 30 min at room temperature. Methylation was performed by adding to the mixtures in the

Table 3 Ternary gradient used for fractionation of RUP oligosaccharides by LC-MS

Time	%A	%B	%C
0–10 min	73–50	2–25	25
10–23.5 min	50–2	25–73	25
23.5–27.5 min	2	73	25

A, pure water; B, pure methanol; and C, 20 mM heptylammonium dissolved in water adjusted to pH 6 by addition of formic acid.

following order: 0.2 ml of NaOH-DMSO reagent and 0.1 ml of methyl iodide (Anumula and Taylor 1992). To enhance the reaction, mixtures were sonicated and vortexed several times. The reaction was stopped after 10 min by the addition of water (2 ml) and the methylated products were extracted with chloroform (2 ml). The solutions were vigorously vortexed before a brief centrifugation, which allowed a strict separation of two phases. The aqueous supernatant phase was removed by aspiration. The organic phase was washed three times with water (2 ml) and dried under a stream of N_2. Methylated carbohydrates were hydrolyzed with 2 M trifluoroacetic acid and converted to their alditol acetates. The partially methylated alditol acetates were analyzed by gas chromatography–mass spectrometry (TRACE-GC-ISQ, Thermo^{TM}) on a non-polar thermo scientific^{TM} TraceGOLD^{TM} TG-1MS GC Column (30 m × 0.25 mm × 0.25 μm) using H_2 as carrier gas at a flow rate of 1.5 ml min^{-1}. The samples were injected at 240°C. The column oven temperature was maintained for 5 min at 60°C and increased up to 315°C (3°C min^{-1}), where it was maintained for 2 min. The ion source temperature of the electron impact (EI) mass spectrometer was 230°C. Masses were acquired with a scan range from *m/z* 100 to 500. Identification of partially methylated alditol acetates was based on their retention time combined with mass spectra fragmentation and compared with a home-made library. Samples were also analyzed on a GC Perkin-Elmer autosystem equipped with a fused-silica capillary column (30 m × 0.32 mm) bound with OV-225 (50% cyanopropylphenyl dimethylpolysiloxane) using H_2 as carrier (80 KPa). Detection was performed at 220°C with a flame ionization detector (FID). The results from both assays were averaged as they closely converged.

Neoglycoprotein preparation

Neoglycoproteins were prepared by coupling RUP oligosaccharides to BSA or ovalbumin by reductive amination (Roy et al. 1984). The relative proportion of carbohydrate to protein in the conjugates was determined using the orcinol and *m*-hydroxybiphenyl methods for carbohydrates (Thibault 1979, Tollier and Robin 1979), and the Bradford method (Bradford 1976) for proteins. The weight ratio of proteins to oligosaccharides was 0.7 for BSA conjugates and 0.43 for ovalbumin conjugates.

Production of antibodies

Three BALB/c mice were injected subcutaneously twice at 2 week intervals with 20 μg of RUP–BSA emulsified in Titermax Gold Adjuvant (Sigma). Three days after the second immunization, mice were sacrificed. The popliteal lymph nodes were removed, and the lymphocytes were suspended by perfusion and fused with a SP2/0 myeloma cell line using standard hybridoma preparation and limiting dilution cloning procedures. The hybridoma supernatants from the fusion were screened for the presence of antibodies reacting with RUP–BSA conjugate by indirect ELISA. The selected hybridomas were subcloned by dilution. Crude hybridoma supernatants were used as the source of monoclonal antibodies.

Indirect ELISA and competitive inhibition ELISA

Indirect ELISA and competitive inhibition ELISA were performed as described in Ralet et al. (2010). RUP and other pectin-derived materials were used as competitors. The concentration of competitor giving a 50% inhibition (IC_{50}) of the binding was determined by plotting the competitor concentration vs. absorbance. Values from controls with no competitor were taken as 0% inhibition, and values from controls with no antibody represented 100% inhibition of binding.

Competitive inhibition ELISA was also performed using as competitors RUP oligosaccharide fractions separated by anion-exchange chromatography. Each fraction was diluted 5-fold with 25 mM Na-acetate buffer to obtain a 1 ml final volume. The pH of phosphate-buffered saline (PBS) buffer was adjusted to pH 8 (PBS8) to balance the acidic acetate buffer (pH 5.5) present in the fractions. KCl concentration was also increased to 5.4 mM in PBS8. The fractions were finally diluted 2-fold with PBS8. A 50 μl aliquot of the diluted solutions (containing carbohydrates) was mixed with 50 μl of clone supernatant. The following steps were performed as described above. Pools (P1–P5) were considered for further characterization. Pools were collected, dialyzed and desalted using a column (100 × 1.6 cm) of Sephadex G-10 at 1 ml min^{-1} eluted with deionized water and then freeze-dried.

Glycan microarray

Polysaccharides and oligosaccharides derived from different pectin and hemicellulose sources were used to evaluate the mAb binding specificities (Moller et al. 2008, Sørensen et al. 2009, Pedersen et al. 2012). Polysaccharides were dissolved in water. Oligosaccharides were coupled to BSA (Roy et al. 1984, Pedersen et al. 2012). Glycans and glycoconjugates were printed using a piezoelectric non-contact microarray robot (Sprint, Arrayjet) onto a nitrocellulose membrane with a pore size of 0.45 μm (Whatman). The developed microarrays were scanned at 2,400 d.p.i. (CanoScan 8800F), converted to TIFFs and signals were measured using Array-Pro Analyzer 6.3 (Media Cybernetics software). The mean spot signals obtained are presented in a heatmap in which the color intensity is correlated to signal. The highest signal in each data set was set to 100, and all other values were normalized accordingly, as indicated by the color scale bar.

LC-MS

Ion pairing-reversed phase chromatography separation (IP-RP-UHPLC). Chromatographic separation of RUP samples and P1–P5 was achieved at 45°C, on an ultra-performance liquid chromatographic system (UHPLC, Acquity H-Class® Waters), mounted with a BEH C18 column (100 × 1 mm, packed with 1.7 μm porosity particles; Waters), at a flow rate of 150 ml min^{-1}. A ternary gradient was applied (**Table 3**) as described in Ropartz et al. (2014).

Collision-induced dissociation (CID) MS/MS measurements. MS/MS experiments were performed on a Q-TOF Synapt G2Si HDMS (Waters) in negative ion mode. Samples were diluted 2-fold with MeOH introduced manually into the electrospray ion source at a flow rate of 5 ml min^{-1}. The ion spray capillary voltage was maintained at 3 kV and the temperature source at 120°C. Argon was used as collision gas. Collision energy was optimized for each sample. Fragments were annotated according to the nomenclature of Domon and Costello (1988). Data were recorded using MassLynx 4.1 (Waters).

Immunofluorescence microscopy

Sample preparation. Small pieces of fresh tissues were sampled from peripheral regions of potato tubers and elongation zones of carrot roots. Samples for light microscopy and transmission electron microcopy (TEM) were processed as described in Ralet et al. (2010). Semi-thin (1 μm) and ultra-thin sections (80 nm) were cut with an ultramicrotome (Leica Microsystems, UC7) equipped with a diamond knife. Semi-thin sections were mounted on multiwell glass sides pre-treated with VectaBond section adhesive (Vector Laboratories, www.vectorlabs.com). Ultra-thin sections were collected on nickel grids.

Toluidine blue staining. Semi-thin sections were stained with 1% (w/v) toluidine blue O in 2.5% Na_2CO_3 for 60 s then washed with water and examined with a microscope (Zeiss, Axiovert-135) equipped with a QImaging Retiga 2000R Scientific CCD Camera.

Immunolabeling. Sections were subjected to immunofluorescence and immunogold labeling. The sections were treated with 3% BSA in PBS for 1 h at room temperature to block non-specific labeling. Then, material was incubated for 1 h at room temperature with primary LM5 (Jones et al. 1997), LM6 (Willats

et al. 1998), INRA-RU1 (Ralet et al. 2010) and INRA-AGI-1 hybridoma supernatants at dilutions of 1/10 in PBS containing 1% BSA and 0.05% Tween (BT-PBS). Tissues were washed (five times for 5 min) in BT-PBS and then exposed to goat anti-rat (LM5, LM6) or anti-mouse (INRA-RU1, INRA-AGI-1) IgG antibodies conjugated to Alexa fluor® 546 nm at a dilution of 1/100 in BT-PBS for 1 h. The samples were washed three times in BT-PBS and five times in water. For the immunofluorescence, sections were covered with water, mounted with a cover slide and observed using a microscope (Leica, DMRD) equipped with epifluorescence irradiation. A band-pass filter at 515–560 nm was used as the excitation filter and fluorescence was detected at >570 nm. Images were recorded with a sensitive cooled camera (Nikon, DS-1QM). For TEM, sections were treated following the same procedure as that of resin-embedded semi-thin sections, using as secondary mAbs nanogold conjugates (goat anti-rat IgG or goat anti-mouse IgG conjugated with 1 nm colloidal gold complexes, Aurion) diluted 1:20 (v/v) in the buffer used for diluting the primary antibodies. Labeling was intensified with silver enhancement kits (Aurion) according to the manufacturer's instructions. Sections were stained with 2% uranyl acetate and then examined with a transmission electron microscope (Jeol, JEM-1230) with an accelerating voltage of 80 kV. In some cases, enzymatic treatments were applied on sections prior to immunolabeling. RGI was degraded using endo-arabinanase (2 U), endo-galactanase (2 U), rhamnogalacturonan hydrolase (0.1 mg ml^{-1}) and pectin lyase (1.4 nKat) in 50 mM acetate buffer pH 4.5, for one night at 37°C. For multi-treatment on the same cross-section, each enzyme was applied sequentially, in the following order: (i) endogalactanase; (ii) endoarabinanase; and (iii) finally rhamnogalacturonane hydrolase or pectin lyase. After and between each enzymatic treatment, samples were washed first with 50 mM acetate buffer pH 4.5 (five times for 5 min) and then with water (three times for 5 min).

Supplementary data

Supplementary data are available at PCP online.

Funding

This work was supported by the European Union [Seventh Framework Programme (FP7 2007–2013) under 'Grant Agreement No. 263916']; Innovation Fund Denmark [as part of the GlycACT project (0603-00417B) (M.G.R.)]. This article reflects the author's views only. The European Community is not liable for any use that may be made of the information contained herein.

Acknowledgements

The authors thank Marie-Jeanne Crépeau for general help and fruitful discussions, Jacqueline Vigouroux for her assistance in the sugar linkage analysis work, and Guy Chevalier for kindly providing carrots.

Disclosures

The authors have no conflicts of interest to declare.

References

Albersheim, P., Darvill, A.G., O'Neill, M.A., Schols, H.A. and Voragen, A.G.J. (1996) An hypothesis: the same six polysaccharides are components of the primary cell wall of all higher plants. *In* Pectins and Pectinases. Edited by Visser, J. and Voragen, A.G.J. pp. pp. 47–53. Elsevier, Amsterdam.

Anumula, K.R. and Taylor, P.B. (1992) A comprehensive procedure for preparation of partially methylated alditol acetates from glycoprotein carbohydrates. *Anal. Biochem.* 203: 101–108.

Bonnin, E., Dolo, E., Le Goff, A. and Thibault, J.-F. (2002) Characterisation of pectin subunits released by an optimised combination of enzymes. *Carbohydr. Res.* 337: 1687–1696.

Bradford, M.M.A. (1976) A rapid and sensitive method for the quantification of the protein utilizing the principle of protein–dye binding. *Anal. Biochem.* 72: 248–255.

Buckeridge, M.S., Hutcheon, I.S. and Reid, J.S. (2005) The role of exo-(1→4)-beta-galactanase in the mobilization of polysaccharides from the cotyledon cell walls of *Lupinus angustifolius* following germination. *Ann. Bot.* 96: 435–444.

Bush, M.S., Marry, M., Huxham, I.M., Jarvis, M.C. and McCann, M.C. (2001) Developmental regulation of pectic epitopes during potato tuberisation. *Planta* 213: 869–880.

Bush, M.S. and McCann, M.C. (1999) Pectic epitopes are differentially distributed in the cell walls of potato (Solanum tuberosum) tubers. *Physiol. Plant.* 107: 201–213.

Caffall, K.H. and Mohnen, D. (2009) The structure, function, and biosynthesis of plant cell wall pectic polysaccharides. *Carbohydr. Res.* 344: 1879–1900.

Carpita, N.C. and Gibeaut, D.M. (1993) Structural models of primary cell walls in flowering plants: consistency of molecular structure with the physical properties of the walls during growth. *Plant J.* 3: 1–30.

Clausen, M.H., Ralet, M.-C., Willats, W.G.T., McCartney, L., Marcus, S.E., Thibault, J.-F., et al. (2004) A monoclonal antibody to feruloylated-(1→4)-β-D-galactan. *Planta* 219: 1036–1041.

Clausen, M.H., Willats, W.G. and Knox, J.P. (2003) Synthetic methyl hexagalacturonate hapten inhibitors of anti-homogalacturonan monoclonal antibodies LM7, JIM5 and JIM7. *Carbohydr. Res.* 338: 1797–1800.

Colquhoun, I.J., de Ruiter, G.A., Schols, H.A. and Voragen, A.G. (1990) Identification by NMR spectroscopy of oligosaccharides obtained by treatment of the hairy regions of apple pectin with rhamnogalacturonase. *Carbohydr. Res.* 206: 131–144.

Cornuault, V., Manfield, I.W., Ralet, M.C. and Knox, J.P. (2014) Epitope detection chromatography: a method to dissect the structural heterogeneity and inter-connections of plant cell-wall matrix glycans. *Plant J.* 78: 715–722.

Cornuault, V., Buffetto, F., Rydahl, M.G., Marcus, S.E., Torode, T.A., Xue, J., et al. (2015) Monoclonal antibodies indicate low-abundance links between heteroxylan and other glycans of plant cell walls. *Planta* 242: 1321–1334.

Domon, B. and Costello, C.E. (1988) A systematic nomenclature for carbohydrate fragmentations in FAB-MS/MS spectra of glycoconjugates. *Glycoconjugate J.* 5: 397–409.

Ducasse, M.A., Williams, P., Canal-Llauberes, R.M., Mazerolles, G., Cheynier, V. and Doco, T. (2011) Effect of macerating enzymes on the oligosaccharide profiles of Merlot red wines. *J. Agric. Food Chem.* 59: 6558–6567.

Englyst, H.N. and Cummings, J.H. (1988) Improved method for measurement of dietary fiber as non-starch polysaccharides in plant foods. *J. Assoc. Anal. Chem.* 71: 808–814.

Ermel, F.F., Follet-Gueye, M.L., Cibert, C., Vian, B., Morvan, C., Catesson, A.M., et al. (2000) Differential localization of arabinan and galactan side chains of rhamnogalacturonan 1 in cambial derivatives. *Planta* 210: 732–740.

Gomez, L.D., Steele-King, C.G., Jones, L., Foster, J.M., Vuttipongchaikij, S. and McQueen-Mason, S.J. (2009) Arabinan metabolism during seed development and germination in Arabidopsis. *Mol. Plant* 2: 966–976.

Ha, M.A., Vietor, R.J., Jardine, G.D., Apperley, D.C. and Jarvis, M.C. (2005) Conformation and mobility of the arabinan and galactan side-chains of pectin. *Phytochemistry* 66: 1817–1824.

Harholt, J., Jensen, J.K., Sorensen, S.O., Orfila, C., Pauly, M. and Scheller, H.V. (2006) ARABINAN DEFICIENT 1 is a putative arabinosyltransferase involved in biosynthesis of pectic arabinan in Arabidopsis. *Plant Physiol.* 140: 49–58.

Harholt, J., Jensen, J.K., Verhertbruggen, Y., Sogaard, C., Bernard, S., Nafisi, M., et al. (2012) ARAD proteins associated with pectic arabinan biosynthesis form complexes when transiently overexpressed in planta. *Planta* 236: 115–128.

Herve du Penhoat, C., Michon, V. and Goldberg, R. (1987) Development of arabinans and galactans during the maturation of hypocotyl cells of mung bean (Vigna radiata Wilczek). *Carbohydr. Res.* 165: 31–42.

Huisman, M.M., Brul, L.P., Thomas-Oates, J.E., Haverkamp, J., Schols, H.A. and Voragen, A.G. (2001) The occurrence of internal (1→5)-linked arabinofuranose and arabinopyranose residues in arabinogalactan side chains from soybean pectic substances. *Carbohydr. Res.* 330: 103–114.

Iwai, H., Ishii, T. and Satoh, S. (2001) Absence of arabinan in the side chains of the pectic polysaccharides strongly associated with cell walls of Nicotiana plumbaginifolia non-organogenic callus with loosely attached constituent cells. *Planta* 213: 907–915.

Jarvis, M.C., Hall, M.A., Threlfall, D.R. and Friend, J. (1981) The polysaccharide structure of potato cell walls: chemical fractionation. *Planta* 152: 93–100.

Jones, L., Milne, J.L., Ashford, D., McCann, M.C. and McQueen-Mason, S.J. (2005) A conserved functional role of pectic polymers in stomatal guard cells from a range of plant species. *Planta* 221: 255–264.

Jones, L., Milne, J.L., Ashford, D. and McQueen-Mason, S.J. (2003) Cell wall arabinan is essential for guard cell function. *Proc. Natl Acad. Sci. USA* 100: 11783–11788.

Jones, L., Seymour, G.B. and Knox, J.P. (1997) Localization of pectic galactan in tomato cell walls using a monoclonal antibody specific to (1→4)-[beta]-D-galactan. *Plant Physiol.* 113: 1405–1412.

Khodaei, N. and Karboune, S. (2013) Extraction and structural characterisation of rhamnogalacturonan I-type pectic polysaccharides from potato cell wall. *Food Chem.* 139: 617–623.

Lahaye, M., Vigouroux, J. and Thibault, J.F. (1991) Endo-beta-1,4-D-galactanase from Aspergillus niger var. aculeatus: purification and some properties. *Carbohydr. Polym.* 4: 431–444.

Larsen, F.H., Byg, I., Damager, I., Diaz, J., Engelsen, S.B. and Ulvskov, P. (2011) Residue specific hydration of primary cell wall potato pectin identified by solid-state 13C single-pulse MAS and CP/MAS NMR spectroscopy. *Biomacromolecules* 12: 1844–1850.

Lau, J.M., McNeil, M., Darvill, A.G. and Albersheim, P. (1987) Treatment of rhamnogalacturonan I with lithium in ethylenediamine. *Carbohydr. Res.* 168: 245–274.

Lee, K.J., Cornuault, V., Manfield, I.W., Ralet, M.C. and Knox, J.P. (2013) Multi-scale spatial heterogeneity of pectic rhamnogalacturonan I (RG-I) structural features in tobacco seed endosperm cell walls. *Plant J.* 75: 1018–1027.

Lerouge, P., O'Neill, M.A., Darvill, A.G. and Albersheim, P. (1993) Structural characterization of endo-glycanase-generated oligoglycosyl side chains of rhamnogalacturonan I. *Carbohydr. Res.* 243: 359–371.

Liners, F., Letesson, J.J., Didembourg, C. and Van Cutsem, P. (1989) Monoclonal antibodies against pectin: recognition of a conformation induced by calcium. *Plant Physiol.* 91: 1419–1424.

Liwanag, A.J., Ebert, B., Verhertbruggen, Y., Rennie, E.A., Rautengarten, C., Oikawa, A., et al. (2012) Pectin biosynthesis: GALS1 in Arabidopsis thaliana is a beta-1,4-galactan beta-1,4-galactosyltransferase. *Plant Cell* 24: 5024–5036.

Massiot, P., Rouau, X. and Thibault, J.F. (1988) Structural study of the cell-wall of carrot (Daucus carota L). 1. Isolation and characterization of the cell-wall fibers of carrot. *Carbohydr. Res.* 172: 217–227.

McCartney, L., Ormerod, A.P., Gidley, M.J. and Knox, J.P. (2000) Temporal and spatial regulation of pectic (1→4)-beta-D-galactan in cell walls of developing pea cotyledons: implications for mechanical properties. *Plant J.* 22: 105–113.

McCartney, L., Steele-King, C.G., Jordan, E. and Knox, J.P. (2003) Cell wall pectic (1→4)-β-D-galactan marks the acceleration of cell elongation in the Arabidopsis seedling root meristem. *Plant J.* 33: 447–454.

Mohnen, D. (2008) Pectin structure and biosynthesis. *Curr. Opin. Plant Biol.* 11: 266–277.

Moller, I., Marcus, S.E., Haeger, A., Verhertbruggen, Y., Verhoef, R., Schols, H., et al. (2008) High-throughput screening of monoclonal antibodies against plant cell wall glycans by hierarchical clustering of their carbohydrate microarray binding profiles. *Glycoconjugate J.* 25: 37–48.

Moore, J.P., Farrant, J.M. and Driouich, A. (2008) A role for pectin-associated arabinans in maintaining the flexibility of the plant cell wall during water deficit stress. *Plant Signal. Behav.* 3: 102–104.

Moore, J.P., Nguema-Ona, E.E., Vicre-Gibouin, M., Sorensen, I., Willats, W.G., Driouich, A., et al. (2013) Arabinose-rich polymers as an evolutionary strategy to plasticize resurrection plant cell walls against desiccation. *Planta* 237: 739–754.

Ng, J.K., Schroder, R., Sutherland, P.W., Hallett, I.C., Hall, M.I., Prakash, R., et al. (2013) Cell wall structures leading to cultivar differences in softening rates develop early during apple (Malus×domestica) fruit growth. *BMC Plant Biol.* 13: 183.

ØBro, J., Borkhardt, B., Harholt, J., Skjot, M., Willats, W.G. and Ulvskov, P. (2009) Simultaneous in vivo truncation of pectic side chains. *Transgenic Res.* 18: 961–969.

Oomen, R.J.F.J., Doeswijk-Voragen, C.H.L., Bush, M.S., Vincken, J.-P., Borkhardt, B., Van Den Broek, L.A.M., et al. (2002) In muro fragmentation of the rhamnogalacturonan I backbone in potato (Solanum tuberosum L.) results in a reduction and altered location of the galactan and arabinan side-chains and abnormal periderm development. *Plant J.* 30: 403–413.

Orfila, C., Seymour, G.B., Willats, W.G.T., Huxham, I.M., Jarvis, M.C., Dover, C.J., et al. (2001) Altered middle lamella homogalacturonan and disrupted deposition of (1→5)-alpha-L-arabinan in the pericarp of Cnr, a ripening mutant of tomato. *Plant Physiol.* 126: 210–221.

Pedersen, H.L., Fangel, J.U., McCleary, B., Ruzanski, C., Rydahl, M.G., Ralet, M.C., et al. (2012) Versatile high resolution oligosaccharide microarrays for plant glycobiology and cell wall research. *J. Biol. Chem.* 287: 39429–39438.

Ralet, M.C., Dronnet, V., Buchholt, H.C. and Thibault, J.F. (2001) Enzymatically and chemically de-esterified lime pectins: characterisation, polyelectrolyte behaviour and calcium binding properties. *Carbohydr. Res.* 336: 117–125.

Ralet, M.-C., Crépeau, M.-J., Buchholt, H.-C. and Thibault, J.-F. (2003) Polyelectrolyte behaviour and calcium binding properties of sugar beet pectins differing in their degrees of methylation and acetylation. *Biochem. Eng. J.* 16: 191–201.

Ralet, M.C., Tranquet, O., Poulain, D., Moise, A. and Guillon, F. (2010) Monoclonal antibodies to rhamnogalacturonan I backbone. *Planta* 231: 1373–1383.

Ralet, M.-C., Williams, M.A.K., Tanhatan-Nasseri, A., Ropartz, D., Quemener, B. and Bonnin, E. (2012) Innovative enzymatic approach to resolve homogalacturonans based on their methylesterification pattern. *Biomacromolecules* 13: 1615–1624.

Renard, C.M., Crepeau, M.J. and Thibault, J.F. (1999) Glucuronic acid directly linked to galacturonic acid in the rhamnogalacturonan backbone of beet pectins. *Eur. J. Biochem.* 266: 566–574.

Ridley, B.L., O'Neill, M.A. and Mohnen, D.A. (2001) Pectins: structure, biosynthesis, and oligogalacturonide-related signaling. *Phytochemistry* 57: 929–967.

Ropartz, D., Lemoine, J., Giuliani, A., Bittebiere, Y., Enjalbert, Q., Antoine, R., et al. (2014) Deciphering the structure of isomeric oligosaccharides in a complex mixture by tandem mass spectrometry: photon activation with vacuum ultra-violet brings unique information and enables definitive structure assignment. *Anal. Chim. Acta* 807: 84–95.

Roy, R., Katzenellenbogen, E. and Jennings, H.J. (1984) Improved procedures for the conjugation of oligosaccharides to protein by reductive amination. *Can. J. Biochem. Cell Biol.* 62: 270–275.

Sabba, R.P. and Lulai, E.C. (2004) Immunocytological comparison of native and wound periderm maturation in potato tuber. *Amer. J. Potato Res.* 81: 119–124.

Schols, H.A. and Voragen, A.G.J. (1994) Occurrence of pectic hairy regions in various plant cell wall materials and their degradability by rhamnogalacturonase. *Carbohydr. Res.* 256: 83–95.

Schols, H.A., Voragen, A.G. and Colquhoun, I.J. (1994) Isolation and characterization of rhamnogalacturonan oligomers, liberated during degradation of pectic hairy regions by rhamnogalacturonase. *Carbohydr. Res.* 256: 97–111.

Skjøt, M., Pauly, M., Bush, M.S., Borkhardt, B., McCann, M.C. and Ulvskov, P. (2002) Direct interference with rhamnogalacturonan I biosynthesis in Golgi vesicles. *Plant Physiol.* 129: 95–102.

Sørensen, I., Pedersen, H.L. and Willats, W.G.T. (2009) An array of possibilities for pectin. *Carbohydr. Res.* 344: 1872–1878.

Sørensen, S.O., Pauly, M., Bush, M., Skjot, M., McCann, M.C., Borkhardt, B., et al. (2000) Pectin engineering: modification of potato pectin by in vivo expression of an endo-1,4-beta-D-galactanase. *Proc. Natl Acad. Sci. USA* 97: 7639–7644.

Tan, L., Eberhard, S., Pattathil, S., Warder, C., Glushka, J., Yuan, C.H., Hao, Z.Y., Zhu, X., Avci, U., Miller, J.S., Baldwin, D., Pham, C., Orlando, R., Darvill, A., Hahn, M.G., Kieliszewski, M.J., Mohnen, D. (2013) An Arabidopsis Cell Wall Proteoglycan Consists of Pectin and Arabinoxylan Covalently Linked to an Arabinogalactan Protein. *Plant Cell.* 25: 270–287.

Tanhatan-Nasseri, A., Crépeau, M.-J., Thibault, J.-F.O. and Ralet, M.-C. (2011) Isolation and characterization of model homogalacturonans of tailored methylesterification patterns. *Carbohydr. Polym.* 86: 1236–1243.

Thibault, J.F. (1979) Automatisation du dosage des substances pectiques par la methode au méta-hydroxydiphényle. *Lebensm.-Wiss. Technol.* 71: 215–223.

Tollier, M.T. and Robin, J.P. (1979) Adaptation de la méthode à l'orcinol sulfurique au dosage automatique des glucides neutres totaux: conditions d'application aux extraits d'origine végétale. *Ann. Technol. Agric.* 28: 1–15.

Ulvskov, P., Wium, H., Bruce, D., Jørgensen, B., Qvist, K.B., Skjøt, M., et al. (2005) Biophysical consequences of remodeling the neutral side chains of rhamnogalacturonan I in tubers of transgenic potatoes. *Planta* 220: 609–620.

Verhertbruggen, Y., Marcus, S.E., Haeger, A., Ordaz-Ortiz, J.J. and Knox, J.P. (2009b) An extended set of monoclonal antibodies to pectic homogalacturonan. *Carbohydr. Res.* 344: 1858–1862.

Verhertbruggen, Y., Marcus, S.E., Haeger, A., Verhoef, R., Schols, H.A., McCleary, B.V., et al. (2009a) Developmental complexity of arabinan polysaccharides and their processing in plant cell walls. *Plant J.* 59: 413–425.

Verhertbruggen, Y., Marcus, S.E., Chen, J. and Knox, J.P. (2013) Cell wall pectic arabinans influence the mechanical properties of Arabidopsis thaliana inflorescence stems and their response to mechanical stress. *Plant Cell Physiol.* 54: 1278–1288.

Willats, W.G., Steele-King, C.G., Marcus, S.E. and Knox, J.P. (1999) Side chains of pectic polysaccharides are regulated in relation to cell proliferation and cell differentiation. *Plant J.* 20: 619–628.

Willats, W.G.T., Marcus, S.E. and Knox, J.P. (1998) Generation of a monoclonal antibody specific to (1→5)-α-L-arabinan. *Carbohydr. Res.* 308: 149–152.

Willats, W.G.T., McCartney, L., Mackie, W. and Knox, J.P. (2001) Pectin: cell biology and prospects for functional analysis. *Plant Mol. Biol.* 47: 9–27.

Young, R.E., McFarlane, H.E., Hahn, M.G., Western, T.L., Haughn, G.W. and Samuels, A.L. (2008) Analysis of the Golgi apparatus in Arabidopsis seed coat cells during polarized secretion of pectin-rich mucilage. *Plant Cell* 20: 1623–1638.

Zheng, Y. and Mort, A. (2008) Isolation and structural characterization of a novel oligosaccharide from the rhamnogalacturonan of Gossypium hirsutum L. *Carbohydr. Res.* 343: 1041–1049.

Zykwinska, A., Ralet, M.C., Garnier, C.D. and Thibault, J.F. (2005) Evidence for in vitro binding of pectin side chains to cellulose. *Plant Physiol.* 139: 397–407.

Zykwinska, A., Rondeau-Mouro, C., Garnier, C., Thibault, J.F. and Ralet, M.C. (2006) Alkaline extractability of pectic arabinan and galactan and their mobility in sugar beet and potato cell walls. *Carbohydr. Polym.* 65: 510–520.

Zykwinska, A., Thibault, J.F. and Ralet, M.C. (2007) Organization of pectic arabinan and galactan side chains in association with cellulose microfibrils in primary cell walls and related models envisaged. *J. Exp. Bot.* 58: 1795–1802.